Science

REPORTS

Cite as: P. Li *et al.*, *Science* 10.1126/science.aam7851 (2017).

Bottom-up construction of a superstructure in a porous uranium-organic crystal

Peng Li,[1] Nicolaas A. Vermeulen,[1] Christos D. Malliakas,[1] Diego A. Gómez-Gualdrón,[2] Ashlee J. Howarth,[1] B. Layla Mehdi,[3] Alice Dohnalkova,[4] Nigel D. Browning,[3,5] Michael O'Keeffe,[6] Omar K. Farha[1,7]*

[1]Department of Chemistry, Northwestern University, Evanston, IL 60208, USA. [2]Chemical and Biological Engineering Department, Colorado School of Mines, Golden, CO 80401, USA. [3]Physical and Computational Science Directorate, Pacific Northwest National Laboratory, Richland, WA 99352, USA. [4]Environmental Molecular Sciences Laboratory, Pacific Northwest National Laboratory, Richland, WA 99352, USA. [5]Materials Science and Engineering, University of Washington, Seattle, WA 98195, USA. [6]School of Molecular Sciences, Arizona State University, Tempe, AZ 85287, USA. [7]Department of Chemistry, Faculty of Science, King Abdulaziz University, Jeddah, Saudi Arabia.

***Corresponding author. Email: o-farha@northwestern.edu**

Bottom-up construction of highly intricate structures from simple building blocks remains one of the most difficult challenges in chemistry. Here, we report a structurally complex, mesoporous uranium-based metal-organic framework (MOF) made from simple starting components. The structure is comprised of 10 uranium nodes and 7 tricarboxylate ligands (both crystallographically non-equivalent); resulting in a 173.3 angstrom cubic unit cell enclosing 816 uranium nodes and 816 organic linkers—the largest unit cell found for any nonbiological material. The cuboctahedra organize into pentagonal and hexagonal prismatic secondary structures which then form tetrahedral and diamond quaternary topologies with unprecedented complexity. This packing results in the formation of colossal icosidodecahedral and rectified hexakaidecahedral cavities with internal diameters of 5.0 nm and 6.2 nm, respectively—ultimately giving rise to the lowest density MOF reported to date.

The natural and spontaneous assembly of multiple protein chains (each composed of hundreds of amino acids) into giant, precise, complex, and functional secondary, tertiary, and quaternary structures has inspired scientists to study mechanisms of "folding" and "self-assembly" (*1*–*5*). Crystal engineering has enabled synthetic chemists to mimic virus-like discrete polyhedral structures, with upwards of 100 components, through supramolecular assembly from predesigned units (*6*, *7*). A longstanding challenge however, is the creation of complex synthetic assemblies composed of small and simple building units which combine to form extremely complex superstructures, reminiscent of proteins (*8*). Here we show a hierarchical, mesoporous uranium-based metal-organic framework (MOF), NU-1301, with unparalleled structural complexity giving rise to a new three-dimensional net, herein named **nun** (Northwestern University net) and now added to the reticular chemistry structure resource (RCSR) database (*9*). The structure is composed of cuboctahedra which exclusively share triangular faces to form secondary prisms, tertiary cages, and quaternary tetrahedra to give a channel system with diamond topology. The unit cell of NU-1301 is comprised of 816 U nodes and 816 organic linkers therefore giving rise to the largest unit cell reported for any non-biological structure. Built from only single U atom nodes and a topologically simple tritopic linker (Fig. 1), the net is highly intricate with 17 topologically-distinct nodal vertices and 18 discrete edges. Although comprised of U atom nodes, NU-1301 has the lowest framework density (0.124 g/cm^3; H^+ counterion, see table S3) of any MOF reported to date owing—at least in part—to the large void space engendered by the colossal cages formed by the packing of secondary prismatic structures. In addition to the beautiful and highly intricate structure of NU-1301, we also show that the pores are accessible and can be used to selectively adsorb organic molecules and biomolecules with different shapes, dimensions, and charges.

To unveil the structure of NU-1301, we were focused on creating cuboctahedral structures which pack in space by only sharing triangular faces. Packing regular shapes in space is one of the oldest mathematical problems and only a few perfect space-filling polyhedra have been proven theoretically (*10*, *11*). A cuboctahedron is a polyhedron with eight triangular faces and six square faces, which when packed sharing triangular faces give prismatic structures with empty cages (pores). In our conceptual design, the cuboctahedron vertices are provided by the center of the tricarboxylate ligands and the triangular faces correspond to the UO_2 nodes (centered at each face). The triangular uranium nodes, $[UO_2(RCOO)_3]^-$, are generated in situ and represent the most common geometry among uranium (VI) carboxylate complexes (over 570 compounds to date based on Cambridge Structural Database (CSD)) formed by uranyl (UO_2^{2+}) and carboxylate ligands (*12*). (Fig. 1A). These same triangular nodes, $[UO_2(RCOO)_3]^-$, were used as building

blocks to construct NU-1300 by using tetratopic linkers to give a 4,3-connected framework with *tbo* topology (*13*). We expected that the assembly of $[UO_2(RCOO)_3]^-$ nodes, and a tritopic linker with three benzoic acid groups orthogonal to the center benzene ring could realize a 3D structure consisting of cuboctahedral cages exclusively sharing triangular faces (Fig. 1B). The regular dihedral angle between triangular and square faces (α, Fig. 1C) in cuboctahedra is approximately 125.26°; and consequently, the angle left as β when two cuboctahedra pack together by sharing a triangular face is 109.48° (360-2 × α). The angle of 109.48° however, is symmetrically forbidden to allow for the formation of any regular polygons, but with appropriate distortions, the cuboctahedra can pack into secondary structures with either C_5 (α = 126 and β = 108) or C_6 (α = 120 and β = 120) rotational symmetry (Fig. 1C). Given that local 5-fold rotations are incompatible with periodicity (*14*), we could predict that the tertiary structure could not be formed solely using pentagonal prisms to achieve long-range translational symmetry (*15*). Although we could imagine that both secondary pentagonal and hexagonal prisms (Fig. 1C) would form in situ using the simple buildings blocks employed (Fig. 1A), the ratio of pentagonal:hexagonal prisms and the intricate manner in which they would pack was unanticipated (Fig. 1D).

Polyhedral-like yellow crystals of NU-1301 are made by generating the $[UO_2(RCOO)_3]^-$ nodes in situ by reacting uranyl nitrate (50.2 mg, 0.1 mmol) and the tritopic linker 5′-(4-carboxyphenyl)-2′,4′,6′-trimethyl-[1,1′:3′,1″-terphenyl]-4,4″-dicarboxylic acid (**L**) (48.0 mg, 0.1 mmol) in *N*,*N*′-dimethyl formamide (DMF) (5 mL) in the presence of trifluoroacetic acid (TFA) (80 μL, 1.0 mmol) at 120°C for 1 day. Single crystal X-ray diffraction (XRD) was used to help understand the structure of NU-1301 and the initial data collection revealed diffraction from only the U(VI) atoms in the framework. The diffraction pattern observed was indicative of a very large unit cell crystallizing in the cubic *Fd-3m* space group with a unit cell parameter of a = 173.26 Å and volume of 5,201,096 Å^3. The gigantic unit cell size and volume of NU-1301 is, at this point, the largest unit cell reported for a porous crystal—30 times larger than that of the next largest one (*16*)—and more than 500 times larger than the average unit cell based on the CoRE (Computation-Ready, Experimental) MOF database (*17*). For topological density comparison, NU-1301 contains only 0.00941 atoms/Å^3 while diamond contains 0.176 atoms/Å^3. Given the large unit cell and extensive void space of NU-1301, application of conventional small molecule crystallographic methods was inadequate in achieving a structural solution for the framework. Electron density maps only indicate the position of the U atoms while the organic components are not distinguishable from residual solvent in the pores (fig. S1). What can be discerned however, is that i) U atoms are sufficiently far apart to confirm that inorganic MOF nodes are constituted by uranyl (UO_2^{2+}) clusters, and ii) "neighboring" U atoms form equilateral triangles with 17.5 Å sides, consistent with U atoms (located at the triangle vertices) bridged by tricarboxylate linkers (**L**) (whose central ring is located at the triangle centroid). This information can be leveraged to fully elucidate the (3,3)-connected underlying **nun** topological net of NU-1301, which can in turn be used to computationally "synthesize" NU-1301. Indeed, the centroids of the equilateral triangles correspond to the "organic" nodes and were determined using tools available in Materials Studios (*18*). Once the topological net details were complete, we used the net as a blueprint to construct the porous crystal model of NU-1301 in silico using a topologically-based crystal constructor (ToBaCCo) code (*19*) to correctly and efficiently place the 816 uranyl nodes and 816 linkers in the unit cell (fig. S2, see detailed simulation method in supplementary materials). Based on the cuboctahedron concept which only considers the organic nodes as vertices, the structure can be understood as quasi-regular cuboctahedra with diameters of 2.5 nm (Fig. 2A) attached to each neighboring cuboctahedra by sharing a triangular face. As predicted, two kinds of secondary assemblies were formed (Fig. 2B) including a pentagonal prism (with 3.0 nm diameter) assembled by five cuboctahedra and a hexagonal prism (with 3.6 nm diameter) built from six cuboctahedra (Fig. 2B). The unprecedented complexity of the structure begins with the assembly of secondary prisms into two kinds of tertiary structures (Fig. 2C). One is an icosidodecahedron (with 5.0 nm diameter, grey) composed of 20 triangles and 12 pentagons. The other one is a rectified hexakaidecahedron (with 6.2 nm diameter, green) composed of 28 triangles, 12 pentagons and 4 hexagons. Finally, the tertiary structures are interconnected to form two kinds of quaternary superstructures (Fig. 2D). One, a tetrahedral structure composed of icosidodecahedra bridged by pentagonal prisms and the other, a diamond-topology composed of rectified hexakaidecahedra bridged through hexagonal prisms. These two quaternary structures fit together to form a highly complex, ordered and beautiful structure made from two simple components (Fig. 2E).

The net of NU-1301 (**nun**) can be described using tilling with both U and ligand vertices. In the tiling of **nun**, the ligand vertices are the 3-c vertices and the U atoms are the 2-c vertices. There are five different tiles (Fig. 3A). The largest two tiles have the face symbol [10^{12}] (grey) and [$10^{12}.12^4$] (green), which are linked by U vertices making tiles with face symbols [$8^5.10^2$] (yellow) and [$8^6.12^2$] (red). The green tiles are connected with each other through red tiles in a diamond topology (Fig. 3B) and the grey tiles are linked with neighboring grey tiles by yellow tiles in a tetrahedron topology (Fig. 3C). The green and grey tiles are also bridged

via yellow tiles (Fig. 3D). The remaining space is filled by the smallest tile (blue) with face symbol [8^6]. It is worth noting that in the assembled complex structures, the grey and green tiles are spatially arranged in positions similar to that in the simplest and the most common binary structure $MgCu_2$ (Fig. 3E). Each largest tile (green) is surrounded by 28 blue tiles and 12 yellow tiles (yellow) (Fig. 3, F and G).

Further characterization of NU-1301 using a suite of physical methods confirms the highly intricate nature of the structure. For example, thermal gravimetric analysis (TGA) revealed that as-synthesized NU-1301 contains a huge amount of solvent with ~65% weight lost from 80 – 120°C corresponding to both water and DMF (figs. S3 and S4). This large percent weight loss is particularly staggering given that the unit cell of NU-1301 is composed of 816 U atoms. NU-1301 was also found to be thermally stable to temperatures greater than 500°C under both N_2 and air, placing it among the most thermally stable MOFs under these conditions. The porosity of NU-1301 was examined by argon adsorption-desorption experiments performed at 87K (Fig. 4A) (*20*). The Brunauer-Emmett-Teller (BET) surface area calculated from the Ar adsorption isotherm following predetermined consistency criteria (*21*) was found to be 4750 $m^2\ g^{-1}$ (fig. S5A and table S2). The isotherm shape is very unique and contains four easily identifiable steps (plus a fifth smaller step) corresponding to the mesoporous cages in the framework. The easily identifiable steps occur at p/p_0 = 0.15, 0.27, 0.37 and 0.65 with a fifth step beginning at 0.67. These steps are consistent with the sequential filling of the cuboctahedral cages, pentagonal/hexagonal channels, icosidodecahedral cage, and the rectified hexakaidecahedral cages of NU-1301, respectively (Fig. 4A). The experimental pore volume is 3.9 cm^3/g meaning that both the surface area and pore volume of NU-1301 are the highest of all actinide-based MOFs described to date (*17*, *22*) and among the highest of all MOFs (*23*–*27*). The powder X-ray diffraction (PXRD) patterns of as-synthesized and activated NU-1301 match those predicted for the simulated structure and also confirm the phase purity of the bulk material (Fig. 4B). To observe the low angle powder diffraction peaks corresponding to the large unit cell, a combination of transmission geometry and optimized position of the beam stop were utilized. Scanning transmission electron microscopy (STEM) experiments were performed to visualize the cuboctahedral building blocks as well as the high porosity of the sample (fig. S6, see supporting information for details)

In addition to the geometric beauty and complexity of self-assembled superstructures (*28*), porous crystals have captivated the attention of scientists for their potential practical applications. Nanoscale voids inside solid materials that allow guest molecules to be transported, exchanged, and encapsulated (*29*) create opportunities for storing and sorting on the molecular scale. Owing to the anionic uranyl building units in the structure, NU-1301 can be considered an anionic framework which should be able to engage in cation exchange with small organic molecules. To confirm the anionic nature of NU-1301, crystals of the MOF were immersed in DMF solutions containing one of two different small organic molecules: methylene blue (MB, cationic), and resorufin sodium salt (RS, anionic). The change in concentration of each compound in solution was monitored by ultraviolet-visible (UV-Vis) spectroscopy performed on the supernatant. The cationic MB was adsorbed by NU-1301 while the anionic dye remained in solution (fig. S7), thus confirming the anionic nature of the framework. To test the accessibility of the large pores through the 3.1 and 3.6 nm apertures of the framework, uptake of two similar sized proteins, cytochrome *c* (Cyt-*c*, 3.6 × 2.4 × 2.2 nm) and α-lactalbumin (α-La, 4.8 × 1.8 × 1.8 nm), with different isoelectric points (10.3 for Cyt-*c* and 4.5 for α-La) was studied. Given the isoelectric points, the two proteins should carry different surface charges (positive for Cyt-*c* and negative for α-La) in neutral aqueous solution (*13*). As expected, NU-1301 adsorbed the positively charged Cyt-*c* but not the negatively charged α-La (fig. S8) from a neutral aqueous solution. The encapsulation of Cyt-*c* into the mesoporous structure of NU-1301 is further confirmed by confocal laser scanning microscopy (CLSM) (fig. S9) and scanning electron microscopy with energy dispersive X-ray spectroscopy (SEM-EDX) (fig. S10).

Inspired by the uptake of both small and large cationic molecules by NU-1301, two cationic surfactants, one a bearing hydrophilic tail (8-hydroxy-3,6-dioxaoctyltriethylammonium chloride, HDTEA) and the other a hydrophobic tail (trimethylnonylammonium bromide, TMNA) were used to manipulate the hydrophilicity/lipophilicity of the MOF, leading to complexes HDTEA@NU-1301 and TMNA@NU-1301, respectively (fig. S11). Simple tuning of hydrophilicity/lipophilicity of a MOF by postsynthetic modification is of interest for extraction applications in varying media as well as applications in drug delivery, microfluidics and sensing (*30*). The surface wettability of HDTEA@NU-1301 and TMNA@NU-1301 was then characterized using contact-angle measurements (fig. S11, B to E). The contact angle of water and dodecane on HDTEA@NU-1301 is 9 and 135° respectively, indicating the hydrophilic and lipophobic nature of the modified MOF (fig. S11, B and D). In contrast, TMNA@NU-1301 gives a water contact angle of 146° and a dodecane contact angle of 11° confirming the hydrophobic and lipophilic nature of the structure (fig. S11, C and E). These results confirm that the hydrophilicity/lipophilicity of the material can be tuned through cation exchange with a suitably charged surfactant containing ethylene glycol or aliphatic groups respectively. In addition, the porosity of

NU-1301 is maintained after cation exchange with HDTEA and TMNA (figs. S12 and S13). To further demonstrate the hydrophilicity/lipophilicity of HDTEA@NU-1301 and TMNA@NU-1301, the materials were added to a mixture containing equal volumes of hexane and water. When HDTEA@NU-1301 or TMNA@NU-1301 was added to the immiscible mixture, the hydrophilic HDTEA@NU-1301 quickly sinks to the bottom (polar) phase while the lipophilic TMNA@NU-1301 collects in the top (nonpolar) phase (movies S1 and S2).

Using two simple trigonal building blocks, a uranium-based metal-organic framework, NU-1301, with unparalleled structural complexity has been realized. The uranium MOF, NU-1301, represents a new level of functional complexity—with unpredictable quaternary structure complexity—which can be achieved by the use of simple starting materials.

REFERENCES AND NOTES

1. H. Malet, K. Liu, M. El Bakkouri, S. W. Chan, G. Effantin, M. Bacia, W. A. Houry, I. Gutsche, Assembly principles of a unique cage formed by hexameric and decameric *E. coli* proteins. *eLife* **3**, e03653 (2014). Medline
2. S. Nath, R. Banerjee, U. Sen, A novel 8-nm protein cage formed by *Vibrio cholerae* acylphosphatase. *J. Mol. Biol.* **426**, 36–38 (2014). doi:10.1016/j.jmb.2013.09.014 Medline
3. W. R. Wikoff, L. Liljas, R. L. Duda, H. Tsuruta, R. W. Hendrix, J. E. Johnson, Topologically linked protein rings in the bacteriophage HK97 capsid. *Science* **289**, 2129–2133 (2000). doi:10.1126/science.289.5487.2129 Medline
4. Y. Hsia, J. B. Bale, S. Gonen, D. Shi, W. Sheffler, K. K. Fong, U. Nattermann, C. Xu, P.-S. Huang, R. Ravichandran, S. Yi, T. N. Davis, T. Gonen, N. P. King, D. Baker, Design of a hyperstable 60-subunit protein icosahedron. *Nature* **535**, 136–139 (2016). doi:10.1038/nature18010 Medline
5. M. M. Conn, J. Rebek Jr., Self-assembling capsules. *Chem. Rev.* **97**, 1647–1668 (1997). doi:10.1021/cr9603800 Medline
6. Y. Liu, C. Hu, A. Comotti, M. D. Ward, Supramolecular Archimedean cages assembled with 72 hydrogen bonds. *Science* **333**, 436–440 (2011). doi:10.1126/science.1204369 Medline
7. Q.-F. Sun, J. Iwasa, D. Ogawa, Y. Ishido, S. Sato, T. Ozeki, Y. Sei, K. Yamaguchi, M. Fujita, Self-assembled M24L48 polyhedra and their sharp structural switch upon subtle ligand variation. *Science* **328**, 1144–1147 (2010). doi:10.1126/science.1188605 Medline
8. P. F. Damasceno, M. Engel, S. C. Glotzer, Predictive self-assembly of polyhedra into complex structures. *Science* **337**, 453–457 (2012). doi:10.1126/science.1220869 Medline
9. O. Delgado-Friedrichs, S. T. Hyde, M. O'Keeffe, O. M. Yaghi, Crystal structures as periodic graphs: The topological genome and graph databases. *Struct. Chem.* **28**, 39–44 (2016). doi:10.1007/s11224-016-0853-3
10. A. Haji-Akbari, M. Engel, A. S. Keys, X. Zheng, R. G. Petschek, P. Palffy-Muhoray, S. C. Glotzer, Disordered, quasicrystalline and crystalline phases of densely packed tetrahedra. *Nature* **462**, 773–777 (2009). doi:10.1038/nature08641 Medline
11. S. Torquato, Y. Jiao, Dense packings of polyhedra: Platonic and Archimedean solids. *Phys. Rev. E* **80**, 041104 (2009). doi:10.1103/PhysRevE.80.041104 Medline
12. T. Loiseau, I. Mihalcea, N. Henry, C. Volkringer, The crystal chemistry of uranium carboxylates. *Coord. Chem. Rev.* **266–267**, 69–109 (2014). doi:10.1016/j.ccr.2013.08.038
13. P. Li, N. A. Vermeulen, X. Gong, C. D. Malliakas, J. F. Stoddart, J. T. Hupp, O. K. Farha, Design and synthesis of a water-stable anionic uranium-based metal-organic framework (MOF) with ultra large pores. *Angew. Chem. Int. Ed.* **128**, 10514–10518 (2016). doi:10.1002/ange.201605547 Medline
14. D. L. Caspar, E. Fontano, Five-fold symmetry in crystalline quasicrystal lattices. *Proc. Natl. Acad. Sci. U.S.A.* **93**, 14271–14278 (1996). doi:10.1073/pnas.93.25.14271 Medline
15. N. A. Wasio, R. C. Quardokus, R. P. Forrest, C. S. Lent, S. A. Corcelli, J. A. Christie, K. W. Henderson, S. A. Kandel, Self-assembly of hydrogen-bonded two-dimensional quasicrystals. *Nature* **507**, 86–89 (2014). doi:10.1038/nature12993 Medline
16. B. Wang, A. P. Côté, H. Furukawa, M. O'Keeffe, O. M. Yaghi, Colossal cages in zeolitic imidazolate frameworks as selective carbon dioxide reservoirs. *Nature* **453**, 207–211 (2008). doi:10.1038/nature06900 Medline
17. D. Nazarian, J. S. Camp, Y. G. Chung, R. Q. Snurr, D. S. Sholl, Large-scale refinement of metal organic framework structures using DFT. *Chem. Mater.* (2016). 10.1021/acs.chemmater.1026b04226
18. Materials Studio, Accelrys Software Inc., San Diego, CA, 2001–2011.
19. D. A. Gómez-Gualdrón, Y. J. Colón, X. Zhang, T. C. Wang, Y.-S. Chen, J. T. Hupp, T. Yildirim, O. K. Farha, J. Zhang, R. Q. Snurr, Evaluating topologically diverse metal–organic frameworks for cryo-adsorbed hydrogen storage. *Energy Environ. Sci.* **9**, 3279–3289 (2016). doi:10.1039/C6EE02104B
20. M. Thommes, K. Kaneko, A. V. Neimark, J. P. Olivier, F. Rodriguez-Reinoso, J. Rouquerol, K. S. W. Sing, Physisorption of gases, with special reference to the evaluation of surface area and pore size distribution (IUPAC technical report). *Pure Appl. Chem.* **87**, 1051–1069 (2015). doi:10.1515/pac-2014-1117
21. D. A. Gómez-Gualdrón, P. Z. Moghadam, J. T. Hupp, O. K. Farha, R. Q. Snurr, Application of consistency criteria to calculate BET areas of micro- and mesoporous metal-organic frameworks. *J. Am. Chem. Soc.* **138**, 215–224 (2016). doi:10.1021/jacs.5b10266 Medline
22. K.-X. Wang, J.-S. Chen, Extended structures and physicochemical properties of uranyl-organic compounds. *Acc. Chem. Res.* **44**, 531–540 (2011). doi:10.1021/ar200042t Medline
23. O. K. Farha, A. Ö. Yazaydın, I. Eryazici, C. D. Malliakas, B. G. Hauser, M. G. Kanatzidis, S. T. Nguyen, R. Q. Snurr, J. T. Hupp, De novo synthesis of a metal-organic framework material featuring ultrahigh surface area and gas storage capacities. *Nat. Chem.* **2**, 944–948 (2010). doi:10.1038/nchem.834 Medline
24. H. Furukawa, N. Ko, Y. B. Go, N. Aratani, S. B. Choi, E. Choi, A. O. Yazaydin, R. Q. Snurr, M. O'Keeffe, J. Kim, O. M. Yaghi, Ultrahigh porosity in metal-organic frameworks. *Science* **329**, 424–428 (2010). doi:10.1126/science.1192160 Medline
25. O. K. Farha, I. Eryazici, N. C. Jeong, B. G. Hauser, C. E. Wilmer, A. A. Sarjeant, R. Q. Snurr, S. T. Nguyen, A. Ö. Yazaydın, J. T. Hupp, Metal-organic framework materials with ultrahigh surface areas: Is the sky the limit? *J. Am. Chem. Soc.* **134**, 15016–15021 (2012). doi:10.1021/ja3055639 Medline
26. I. Senkovska, S. Kaskel, Ultrahigh porosity in mesoporous MOFs: Promises and limitations. *Chem. Commun.* **50**, 7089–7098 (2014). doi:10.1039/c4cc00524d Medline
27. J. An, O. K. Farha, J. T. Hupp, E. Pohl, J. I. Yeh, N. L. Rosi, Metal-adeninate vertices for the construction of an exceptionally porous metal-organic framework. *Nat. Commun.* **3**, 604 (2012). doi:10.1038/ncomms1618 Medline
28. M. O'Keeffe, M. A. Peskov, S. J. Ramsden, O. M. Yaghi, The Reticular Chemistry Structure Resource (RCSR) database of, and symbols for, crystal nets. *Acc. Chem. Res.* **41**, 1782–1789 (2008). doi:10.1021/ar800124u Medline
29. S. Horike, S. Shimomura, S. Kitagawa, Soft porous crystals. *Nat. Chem.* **1**, 695–704 (2009). doi:10.1038/nchem.444 Medline
30. B. Xin, J. Hao, Reversibly switchable wettability. *Chem. Soc. Rev.* **39**, 769–782 (2010). doi:10.1039/B913622C Medline
31. T. F. Liu, N. A. Vermeulen, A. J. Howarth, P. Li, A. A. Sarjeant, J. T. Hupp, O. K. Farha, Adding to the arsenal of zirconium-based metal-organic frameworks: The topology as a platform for solvent-assisted metal incorporation. *Eur. J. Inorg. Chem.* **2016**, 4349–4352 (2016). doi:10.1002/ejic.201600627
32. T. Shimada, H. Kuyama, T.-A. Sato, K. Tanaka, Development of iodoacetic acid-based cysteine mass tags: Detection enhancement for cysteine-containing peptide by matrix-assisted laser desorption/ionization time-of-flight mass spectrometry. *Anal. Biochem.* **421**, 785–787 (2012). doi:10.1016/j.ab.2011.12.005 Medline

ACKNOWLEDGMENTS

O.K.F. gratefully acknowledges the support from the U.S. DOE, Office of Science, Basic Energy Sciences Program (Grant DE-FG02-08ER155967) and from Northwestern University for the synthesis of the linker, MOF, and MOF characterization. D.A.G-G. gratefully acknowledges the support of the Colorado School of Mines Board of Trustees. A.J.H. thanks NSERC for a postdoctoral fellowship. The X-ray work made use of the IMSERC at Northwestern University, which has received support from the Soft and Hybrid Nanotechnology Experimental (SHyNE) Resource (NSF NNCI-1542205), the State of Illinois, and the International Institute for Nanotechnology (IIN). Computational work made use of the BlueM supercomputer at Colorado School of Mines. STEM experiments were performed by BLM, AD, NDB and were supported by the Chemical Imaging Initiative (CII) Laboratory Directed Research and Development (LDRD) Program at Pacific Northwest National Laboratory (PNNL). PNNL is a multi-program national laboratory operated by Battelle for the U.S. Department of Energy (DOE) under Contract DE-AC05-76RL01830. The STEM work was performed using the Environmental Molecular Sciences Laboratory (EMSL), a national scientific user facility sponsored by the Department of Energy's Office of Biological and Environmental Research and located at PNNL. The authors thank Professor Tobin Marks for providing his facilities for conducting preliminary experiments with uranium. We thank Aaron Peters for help collecting SEM-EDS data. All data and images are available in the body of the paper or as supplementary materials. The x-ray structure is deposited with the Cambridge Crystallographic Data Centre with deposition number 1537423. Author contributions: O.K.F. conceived and initiated the project; P.L. synthesized and characterized and analyzed the gas adsorption, TGA, CLSM, PXRD, elemental analysis, NMR, contact angle data with help from N.A.V. and A.J.H. under the supervision of O.K.F.; N.A.V. prepared the ligand under the supervision of O.K.F. and J.T.H.; C.D.M. collected the single crystal diffraction and solved the U atoms; D.A.G.-G. obtained the topological blueprint and constructed the model porous crystal structure; M.O.; O.K.F. and D.A.G.-G. analyzed the crystal structure and topology; P.L., N.A.V., O.K.F. and A.J.H. wrote the initial paper draft, and all authors contributed to revising the paper.

SUPPLEMENTARY MATERIALS

www.sciencemag.org/cgi/content/full/science.aam7851/DC1
Materials and Methods
Figs. S1 to S17
Tables S1 to S3
Movies S1 and S2
References (*31*, *32*)

16 January 2017; accepted 10 April 2017
Published online 20 April 2017
10.1126/science.aam7851

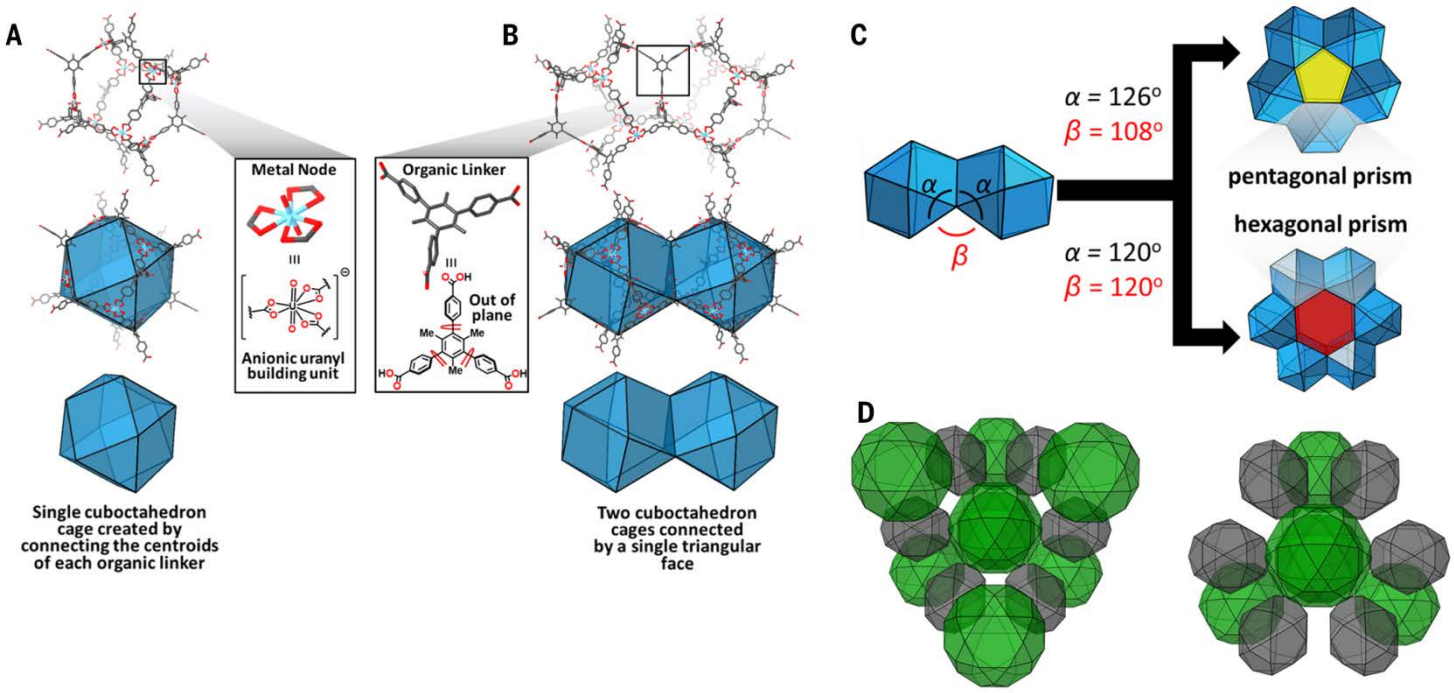

Fig. 1. The cuboctahedron building unit in NU-1301. (**A**) A cuboctahedron built from 8 $[UO_2(RCOO)_3]^-$ units and 12 bridging ligands. (**B**) Two cuboctahedra connected by sharing a single triangular face. (**C**) A pentagonal prism formed by five cuboctahedra and a hexagonal prism formed by six cuboctahedra. (**D**) Different views of the large cage of NU-1301 showing the $MgCu_2$-like structure (green cage for Mg, grey cage for Cu).

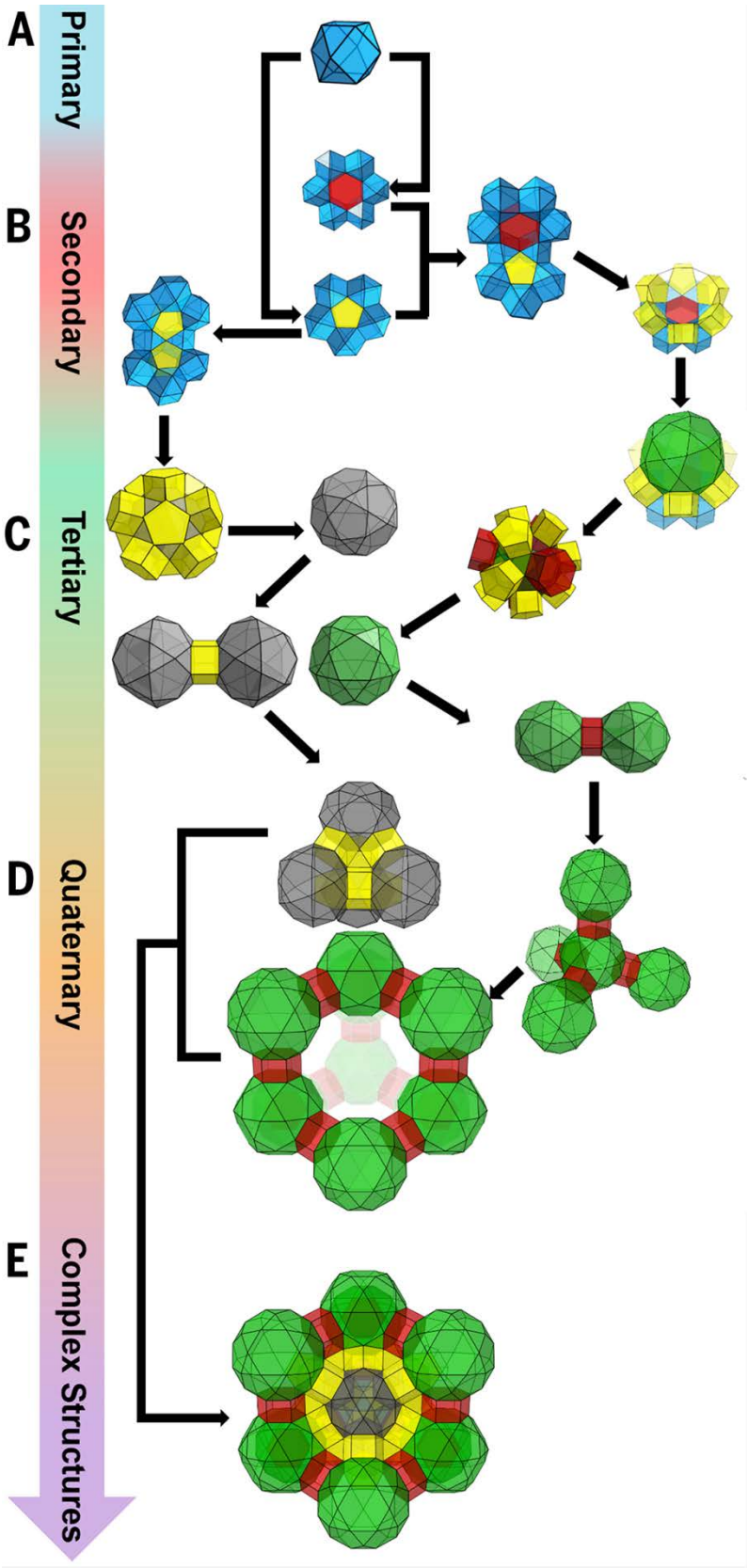

Fig. 2. The arrangement of cuboctahedra into superstructures in NU-1301. (A) Cuboctahedron primary structure. (B) Pentagonal and hexagonal prismatic secondary structures. (C) Icosidodecahedron, and rectified hexakaidecahedron tertiary structures, (D) Tetrahedron and diamond-topology quaternary structures. (E) Complex structure composed of quaternary structures in NU-1301.

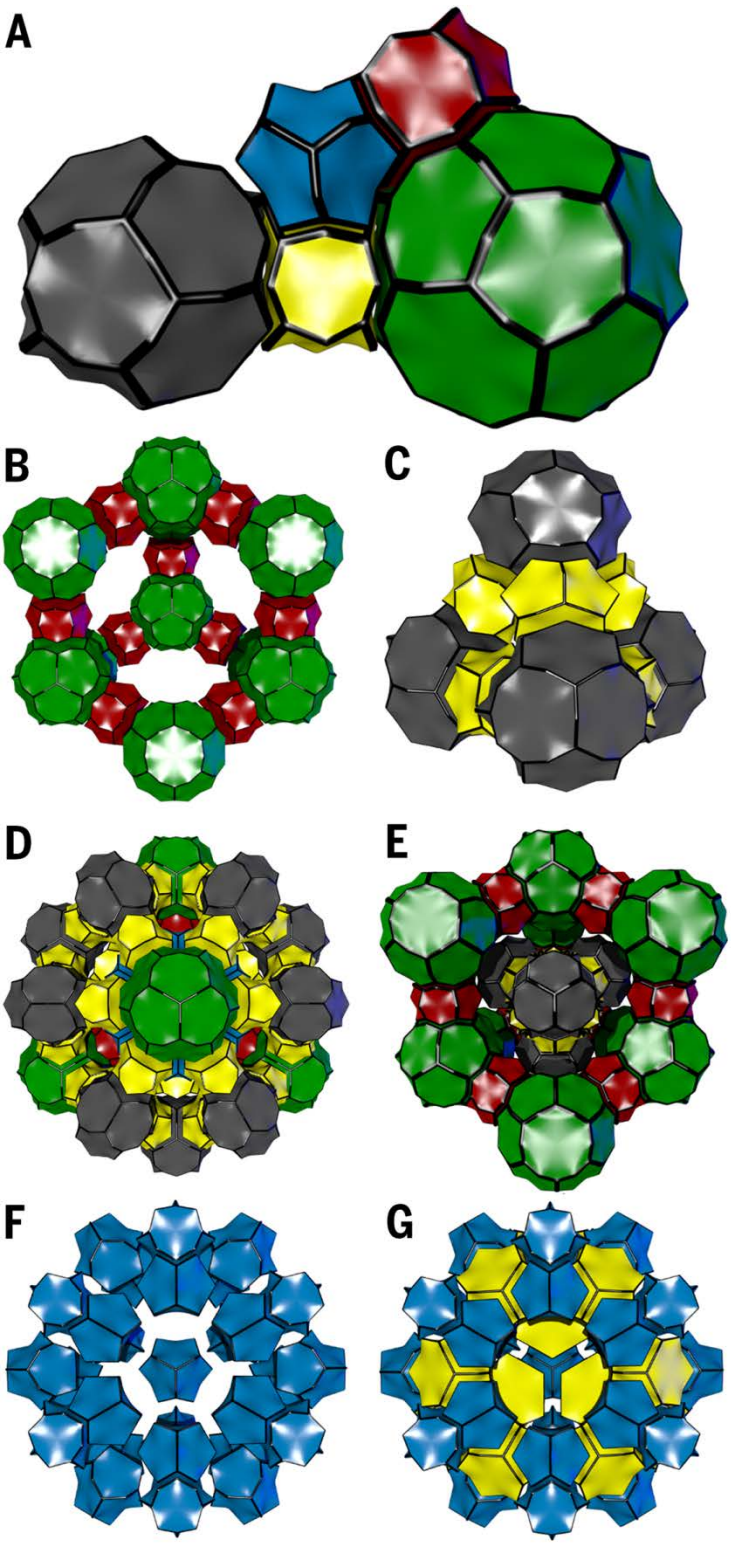

Fig. 3. The *nun* of NU-1301 described by tiling using U atoms and ligand vertices. The face symbols of the five different tiles are $[8^6]$ for blue, $[8^5, 10^2]$ for yellow, $[8^6, 12^2]$ for red, $[10^{12}]$ for grey, and $[10^{12}, 12^4]$ for green.

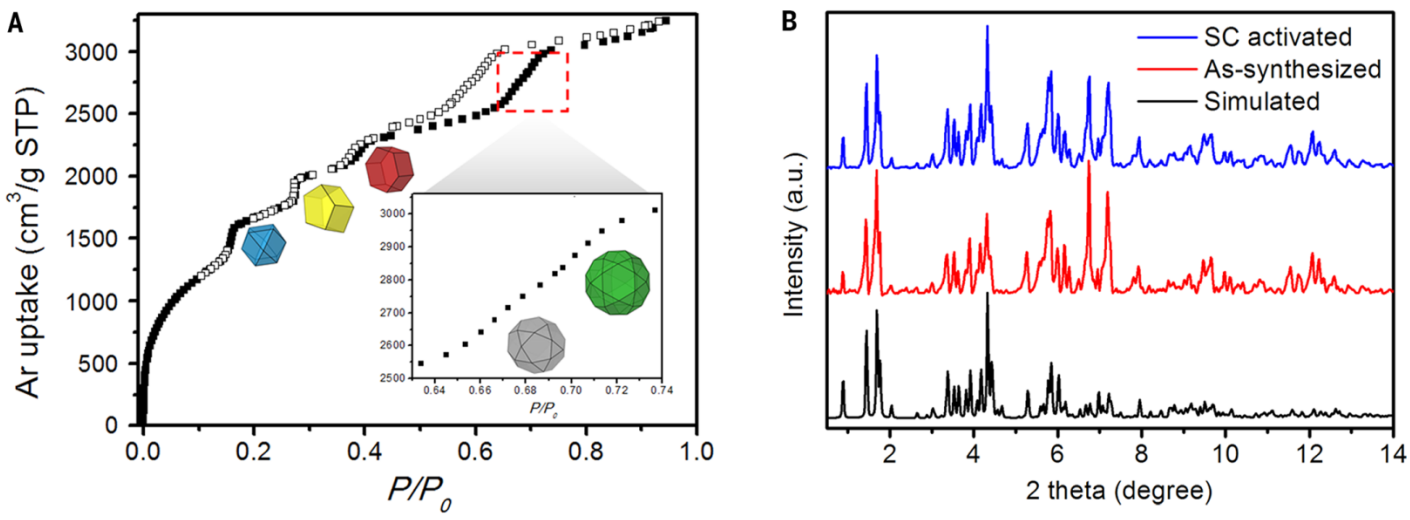

Fig. 4. (A) Ar adsorption/desorption isotherm at 87 K for NU-1301 showing the cages corresponding to the steps in the isotherm. (B) Powder X-ray diffraction patterns of simulated (black), as-synthesized NU-1301 (red) and SC activated NU-1301a (blue).

Bottom-up construction of a superstructure in a porous uranium-organic crystal

Peng Li, Nicolaas A. Vermeulen, Christos D. Malliakas, Diego A. Gómez-Gualdrón, Ashlee J. Howarth, B. Layla Mehdi, Alice Dohnalkova, Nigel D. Browning, Michael O'Keeffe and Omar K. Farha

(April 20, 2017)
published online April 20, 2017

Editor's Summary

Science (print ISSN 0036-8075; online ISSN 1095-9203) is published weekly, except the last week in December, by the American Association for the Advancement of Science, 1200 New York Avenue NW, Washington, DC 20005.